Contribution from the Department of Chemistry,
The University of North Carolina, Chapel Hill, North Carolina 27514

Synthetic Control of Excited States. Nonchromophoric Ligand Variations in Polypyridyl Complexes of Osmium(II)

EDWARD M. KOBER, JANET L. MARSHALL, WALTER J. DRESSICK, B. PATRICK SULLIVAN, JOHNATHAN V. CASPAR, and THOMAS J. MEYER*

Received June 8, 1984

In this paper two themes are explored with regard to the properties of the metal to ligand charge-transfer (MLCT) excited states of Os(II). For a series of Os(II) complexes it is shown that the MLCT excited states undergo facile oxidative or reductive quenching. Excited-state redox potentials have been estimated by both kinetic quenching and spectroscopic techniques for excited-state oxidative couples like $(phen^{-}\cdot)Os^{III}(phen)_2^{2+*} + e^- \rightarrow (phen^{-}\cdot)Os^{II}(phen)_2^{+}$ (phen is 1,10-phenanthroline) and excited-state reductive couples like $(phen^{-}\cdot)Os^{III}(phen)_2^{2+*} \rightarrow Os(phen)_3^{3+} + e^-$. The second theme, the manipulation of excited-state properties by synthetic changes, follows from a consideration of those factors that dictate excited-state redox potentials. It is shown that in the series $(phen)OsL_4^{2+}$ (L = pyridine, CH_3CN, PR_3, AsR_3, ...), where the metal-ligand basis for the MLCT chromophore remains the same and variations are made in the nonchromophoric ligand, emission energies, excited-state redox potentials, and radiative and nonradiative rate constants all vary systematically with the potential of the ground-state Os(III/II) couple. The results show that it is possible through synthetic changes to control excited-state properties in a systematic way.

Introduction

A continuing theme in photochemistry is the use of metal to ligand charge-transfer (MLCT) excited states as sensitizers in a variety of photochemical and photophysical applications.[1-4] One goal of our work is to extend the list of available MLCT excited states by synthetic studies designed to take advantage of variations in the metal, the chromophoric ligand, and the nonchromophoric ligands. In preliminary accounts, we have reported on the lifetime and emission properties of the MLCT excited states of two extended series of complexes of Os(II), $(bpy)OsL_4^{2+}$ and $(phen)OsL_4^{2+}$ (bpy is 2,2'-bipyridine; phen is 1,10-phenanthroline; L is PR_3, AsR_3, pyridine or a substituted pyridine, CH_3CN, ...),[5] and a smaller series of 2,2',2''-terpyridine (trpy) complexes, $Os^{II}(trpy)(diphosphine)L^{n+}$ (diphosphine is $Ph_2PCH_2PPh_2$ or *cis*-$Ph_2PCH{=}CHPPh_2$; L is Cl^- (n = 1) or CH_3CN or pyridine (n = 2)).[6] In the three series the chromophoric basis for the excited state was held constant while variations were made in the remaining, nonchromophoric ligands. The choice of Os over Ru in such studies is dictated in part by the fact that, for polypyridyl complexes of Ru, there are relatively low-lying dd states.[7,8] The dd states provide an additional decay channel, which complicates the interpretation of photophysical properties and, once populated, can lead to photodecomposition.[7-11] In earlier work by Creutz et al., the photophysical properties of the excited states of a smaller series of polypyridine complexes of Os(II) were investigated and it was shown that they undergo facile electron transfer.[12]

The availability of an extended series of electronically related excited states has provided an unprecedented opportunity for exploring the relationship between molecular and electronic structure and the dynamics of excited-state decay. For example, it has been possible to demonstrate the applicability of the energy-gap law to nonradiative decay.[5,9,13,14] However, one of our major interests in preparing a series of related Os-based chromophores was to have access to a family of excited states where excited-state redox potentials could be varied in a systematic manner and over as wide a range as possible. The emphasis on redox potentials follows from the fact that, in the applications involving MLCT excited-states mentioned above, the critical feature, at least initially, is electron-transfer quenching of the excited states.

The work described here includes an extension of the earlier work by Creutz et al.[12] and Crosby et al.[15] on the characterization of Os(II)-based MLCT excited states and is based on two themes. The first is the observation of excited-state electron-transfer reactivity and an estimation of excited-state redox potentials for a variety of Os(II)-based MLCT excited states. The second is based on a second set of complexes where the basis for the chromophore is held constant while variations are made in the nonchromophoric ligands. Here we find that (1) excited-state properties for the Os complexes (lifetimes, redox potentials, radiative quantum yields) can be estimated from a simple electrochemical measurement and that (2) the series of closely related Os complexes represent a class of sensitizers whose properties can be varied systematically and controllably by making variations in the nonchromophoric ligands.

Experimental Section

Materials. Laboratory distilled water was redistilled from alkaline potassium permanganate. Toluene from Fisher Scientific Co. was used as received. Acetonitrile (Matheson Coleman and Bell) was purified by distillation first over P_2O_5 followed by a second distillation over CaH_2. In each case, the first and last 25% fractions were discarded and only the middle 50% fraction was collected. The solvent was stored in a desiccator over $CaCl_2$. Anhydrous $LiClO_4$ (G. Frederick Smith) used without further purification or recrystallized from MeCN gave interchangeable results. Tetraethylammonium perchlorate (TEAP) from Eastman was recrystallized twice from MeCN, dried overnight in an oven at 100 ± 5 °C, and stored in a desiccator over $CaCl_2$.

Oxidative Quenchers. The preparations and purifications of the oxidative quenchers have been described in detail previously.[16] The pyridinium ion products were obtained as chloride or iodide salts and me-

(1) (a) Whitten, D. G. *Acc. Chem. Res.* **1980**, *13*, 83. (b) Meyer, T. J. *Acc. Chem. Res.* **1978**, *11*, 94. (c) Meyer, T. J. *Prog. Inorg. Chem.* **1983**, *30*, 389.
(2) Balzani, V.; Bolleta, F.; Gandolfi, M. T.; Maestri, M. *Top. Curr. Chem.* **1978**, *75*, 1.
(3) (a) Sutin, N.; Creutz, C. *Pure Appl. Chem.* **1980**, *52*, 2717. (b) Sutin, N. *J. Photochem.* **1979**, *10*, 19.
(4) Kalyanasundaram, K. *Coord. Chem. Rev.* **1982**, *46*, 159.
(5) (a) Kober, E. M.; Sullivan, B. P.; Dressick, W. J.; Caspar, J. V.; Meyer, T. J. *J. Am. Chem. Soc.* **1980**, *102*, 1383. (b) Caspar, J. V.; Kober, E. M.; Sullivan, B. P.; Meyer, T. J. *J. Am. Chem. Soc.* **1982**, *104*, 630.
(6) Allen, G. H.; Sullivan, B. P.; Meyer, T. J. *J. Chem. Soc., Chem. Commun.* **1981**, 793.
(7) (a) Van Houten, J.; Watts, R. J. *J. Am. Chem. Soc.* **1976**, *98*, 4853. (b) Van Houten, J.; Watts, R. J. *Inorg. Chem.* **1978**, *17*, 3381.
(8) Durham, B.; Caspar, J. V.; Nagle, J. K.; Meyer, T. J. *J. Am. Chem. Soc.* **1982**, *104*, 4803.
(9) (a) Caspar, J. V.; Meyer, T. J. *Inorg. Chem.* **1983**, *22*, 2444. (b) Caspar, J. W.; Meyer, T. J. *J. Am. Chem. Soc.* **1983**, *105*, 5583.
(10) Gleria, M.; Minto, F.; Baggiato, G.; Bartolus, P. *J. Chem. Soc., Chem. Commun.* **1978**, 285.
(11) (a) Hoggard, P. E.; Porter, G. B. *J. Am. Chem. Soc.* **1978**, *100*, 1457. (b) Wallace, W. M.; Hoggard, P. E. *Inorg. Chem.* **1980**, *19*, 2141.
(12) Creutz, C.; Chou, M.; Netzel, T. L.; Okumura, M.; Sutin, N. *J. Am. Chem. Soc.* **1980**, *102*, 1309.
(13) Caspar, J. V.; Meyer, T. J. *J. Phys. Chem.* **1983**, *87*, 952.
(14) Caspar, J. V.; Kober, E. M.; Sullivan, B. P.; Meyer, T. J. *Chem. Phys. Lett.* **1982**, *91*, 91.
(15) (a) Pankuch, B. J.; Lacky, D. E.; Crosby, G. A. *J. Phys. Chem.* **1980**, *84*, 2061. (b) Lacky, D. E.; Pankuch, B. J.; Crosby, G. A. *Ibid.* **1980**, *84*, 2068.
(16) Nagle, J. K. Ph.D. Dissertation, The University of North Carolina, Chapel Hill, NC, 1979.

0020-1669/85/1324-2755$01.50/0

Table I. Spectroscopic and Excited-State Properties in Acetonitrile Solution

no.	complex[a]	τ_0,[b] ns(deaer)	τ_0,[c] ns(aer)[c]	λ_{max}^{abs},[d] nm	λ_{max}^{em},[e] nm	ϕ_r[f]
1	$Os(trpy)_2^{2+}$	269	<40	698	729	
2	$(trpy)(dppene)OsCl^+$	101	<40	624	718	
3	$Os(phen)_3^{2+}$	262	189	650	720	0.013
4	$(phen)_2Os(MeCN)_2^{2+}$	488	112	600	688	0.035
5	$(phen)_2Os(Me_2PPh)_2^{2+}$	394	214	590	672	0.072
6	$(bpy)_2Os(dppm)^{2+}$	304	185	480	652	0.046
7	$(phen)_2Os(dppm)^{2+}$	1130	233	500	624	0.12
8	$(phen)_2Os(dppene)^{2+}$	1836	367	455	609	0.20
9	$(bpy)Os(das)_2^{2+}$	1640	555	450	592	0.22
10	$(bpy)_2Os(Me_2SO)_2^{2+}$	1500	673	443	575	0.31
11	$(bpy)Os(dppene)_2^{2+}$	1684	1376	400	537	0.41
12	$(3,4,7,8\text{-}Me_4phen)_2Os(dppene)^{2+}$	3462	619	450	594	0.17
13	$Ru(bpy)_3^{2+}$	850	153	452	620	0.062

[a] All complexes as hexafluorophosphate salts. See Table II for ligand abbreviations. [b] Excited-state lifetimes at 23 ± 2 °C; ±5%. Ar-bubble deaeration. [c] Excited-state lifetimes at 23 ± 2 °C; ±5%. Air saturated. [d] Position of the lowest charge-transfer absorption band. [e] Energies at the emission maximum, ±1 nm; corrected for detector response. [f] Radiative quantum yields ±15%.

tathesized to the hexafluorophosphate or tetrafluoroborate salts by addition of the appropriate acid to aqueous solutions containing the cation. The results obtained by using tetrafluoroborate as the anion were identical with those obtained by using hexafluorophosphate as the anion, within experimental error.

Reductive Quenchers. The preparation and purification of tris(*p*-bromophenyl)amine were carried out according to a published procedure.[17] The compounds 2-chlorophenothiazine, 2-(trifluoromethyl)-phenothiazine, 3-methoxyphenothiazine, and phenoxathiin were obtained from ICN Pharmaceuticals, Inc., Plainview, NY, and recrystallized twice from MeCN prior to use. In all cases involving reductive quenchers, the recrystallizations were performed under an argon atmosphere. Samples of both *N,N*-dimethylaniline and *p*-methyl-*N,N*-dimethylaniline were obtained from Aldrich and vacuum distilled under argon before use. Triphenylamine from Aldrich and *p*-bromo-*N,N*-dimethylaniline from Eastern Chemical Co., Hauppage, NY, were recrystallized twice from acetonitrile. Phenothiazine from Aldrich was recrystallized three times from toluene. The remaining reductive quenchers were all from Aldrich and were purified by sublimation immediately prior to use.

Metal Complexes. The preparations of the osmium complexes have been described in preliminary accounts[5] and are described in further detail elsewhere.[18]

Electrochemical Measurements. Electrochemical measurements were performed by using a Princeton Applied Research Model 175 universal programmer and a Model 176 potentiostat. Cyclic voltammetric measurements were performed at 23 ± 2 °C in CH_3CN solution under argon with the electroactive component at 10^{-3} M. Tetraethylammonium perchlorate was used in 0.1 M concentration as the supporting electrolyte with a saturated calomel electrode (SCE) as the reference. Electrochemical reductions of the complexes were performed with use of a Princeton Applied Research Model 179 digital coulometer. The metal complexes were oxidized with PbO_2 (Alfa Ventron).

Because of a lack of suitable reversible couples with appropriate potentials, it was necessary to use several irreversible one-electron quenchers. They were *N*-benzyl-3-carbamidopyridinium hexafluorophosphate, *N*-ethyl-3-carbamidopyridinium hexafluorophosphate, *N,N*-dimethylaniline, and triphenylamine. Although solutions containing these quenchers and the Os(II) complexes were photochromic on the flash photolysis time scale, decomposition was observed on the longer time scale of the cyclic voltammetry experiment. Estimates for the reversible $E^{\circ\prime}$ values for the irreversible quenchers were made by using the method of Olmstead, as described elsewhere.[19]

Quantum Yields. Corrected emission spectra for the Os(II) complexes were obtained with a SLM Instruments Model 8000 spectrofluorimeter and programs provided by the manufacturer. Emission quantum yields for the osmium complexes were determined in CH_3CN at 22 ± 1 °C relative to a solution containing $Ru(bpy)_3^{2+}$ and having the same absorbance. Emission quantum yields for the osmium complexes were determined by comparing integrated emission spectra and using ϕ_{em} = 0.062 (±10%) for the standard.[9]

Flash Photolysis. Flash photolysis experiments were carried out by using solutions 10^{-5}M in osmium complex containing sufficient quencher to quench 95% of the luminescence. Ionic strength was either 0.1 or 0.5 M, adjusted with $LiClO_4$. Solutions were argon bubble degassed for 1 h unless otherwise noted. The flash photolysis spectrometer used has been described previously.[16,20]

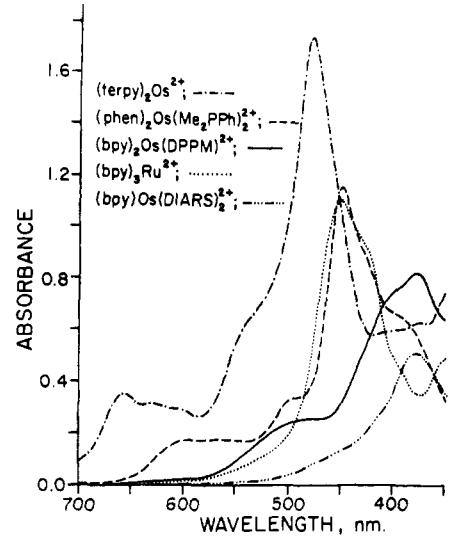

Figure 1. Represntative absorption spectra for Os(II) complexes in acetonitrile (1.00-cm cell): $Os(trpy)_2^{2+}$ (1.10×10^{-4} M); $Os(phen)_2(Me_2PPh)_2^{2+}$ (9.85×10^{-5} M); $Os(bpy)_2(dppm)^{2+}$ (1.30×10^{-4} M); $Ru(bpy)_3^{2+}$ (6.40×10^{-5} M); $Os(bpy)(das)_2^{2+}$ (1.18×10^{-4} M).

Spectra and Quenching Experiments. Absorption spectra of the metal complexes were recorded on a Varian Model 634 UV–vis spectrometer. Absorption spectra for the Os(I) complexes were obtained following electrochemical reduction of Os(II) complexes under an inert atmosphere. Emission intensity measurements for the quencing studies were obtained on a Hitachi Perkin-Elmer MPF-2A spectrofluorimeter. Excitation was from a 150-W Xe lamp and a Hamamastu R-446 red-sensitive photomultiplier tube operated at 750 V as the detector. The bandwidth varied over a range of 5–30 nm depending on the luminescence intensity.

The Stern–Volmer intensity quenching experiments were carried out with argon-degassed solutions and standard techniques as described elsewhere. The values of k_q were calculated from the Stern–Volmer relationship shown in eq 1, where Q is the quencher concentration in M,

$$I_0/I = 1 + k_q\tau_0[Q] \quad (1)$$

I_0/I is the ratio of the luminescence intensities in the absence (I_0) and presence (I) of the quencher and k_q is the quenching rate constant in L mol^{-1} s^{-1}. Excited-state lifetimes (τ_0) were measured by flash photolysis as described previously.[16] Plots of I_0/I vs. $\tau_0[Q]$ were anlyzed by using a weighted, linear-least-squares computer program with the weighting factor $W = I/(1 + I_0/I)$. The slopes of the plots yielded the value of k_q directly. Chemically activated rate constants were calculated from the k_q values after correcting for diffusional contributions.[19] All quenching

(17) Baker, T. N.; Doherty, W. P.; Kelley, W. S.; Newmeyer, W.; Rogers, J. E.; Spalding, R. E.; Walters, R. E. *J. Org. Chem.* **1965**, *30*, 3714.
(18) Kober, E. M.; Sullivan, B. P.; Caspar, J. V.; Meyer, T. J., manuscript in preparation.
(19) Bock, C. R.; Connor, J. A.; Guttierrez, A. R.; Meyer, T. J.; Whitten, D. G.; Sullivan, B. P.; Nagle, J. K. *J. Am. Chem. Soc.* **1979**, *101*, 4815.
(20) (a) Young, R. C.; Keene, F. R.; Meyer, T. J. *J. Am. Chem. Soc.* **1977**, *99*, 2468. (b) Young, R. C.; Nagle, J. K.; Meyer, T. J.; Whitten, D. G. *Ibid.* **1978**, *100*, 4773.

Table II. Ligand Structures and Abbreviations

ligand	abbr	structure
2,2′-bipyridine	bpy	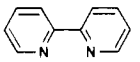
1,10-phenanthroline	phen	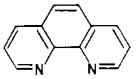
3,4,7,8-tetramethyl-1,10-phenanthroline	Me_4phen	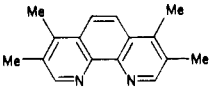
cis-bis(1,2-diphenylphosphino)-ethylene	dppene	
dimethylphenylphosphine	Me_2PPh	Me_2PPh
o-phenylenebis(dimethylarsine)	das	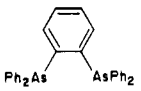
2,2′,2″-terpyridine	trpy	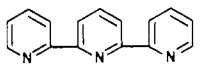
dimethyl sulfoxide	Me_2SO	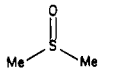
bis(diphenylphosphino)methane	dppm	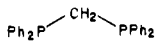
pyridine	py	
bis(1,2-diphenylphosphino)-benzene	dppb	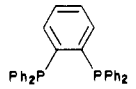
bis(1,2-diphenylarsino)ethane	dpae	$Ph_2AsCH_2CH_2AsPh_2$

data were obtained at 0.1 M ionic strength with the ionic strength adjusted for each solution with $LiClO_4$. Electrochemical measurements on the metal complexes and quenchers made in $LiClO_4$ were consistently 100 mV more negative than the values obtained in 0.1 M TEAP. All of the redox potentials cited here, including the calculated excited-state potentials, are in 0.1 M TEAP–CH_3CN solutions.

Results

Properties of the Os(II) Complexes. Emission and absorption maxima and excited-state photophysical properties are summarized in Table I for several polypyridyl complexes in acetonitrile solution. Absorption spectra are dominated by a series of relatively intense metal to ligand charge-transfer (MLCT) absorptions as shown by the representative spectra in Figure 1. Abbreviations and structures for the organic ligands used in the study are shown in Table II.

Excited-State Quenching and Back Electron Transfer. Reduction potentials for the oxidative and reductive quenchers used to estimate excited-state reduction potentials in acetonitrile are listed in Supplementary Tables I and II. The $E_{1/2}$ values were obtained by cyclic voltammetry. Quenching experiments were carried out in 0.1 M $LiClO_4$–MeCN solution on the excited states of the complexes listed in Table I. Quenching by both sets of oxidative and reductive quenchers in Supplementary Tables I and II was studied for each excited state.

Values for the quenching rate constants, k_q, were calculated with the Stern–Volmer equation (eq 1). Plots of I_0/I vs. $\tau_0[Q]$ were linear over an extended range of quencher concentrations, and the intercepts were unity, as predicted by eq 1, for all complex-quencher pairs studied. Values of k_q and of k_q corrected for diffusional effects, k_q' (note below), are available as Supplementary Tables III and IV.

The results of earlier work on the quenching of $Ru(bpy)_3^{2+*}$ by the same or related quenchers as those used here suggested that quenching was largely by electron transfer rather than energy transfer.[19] We carried out flash photolysis experiments both to obtain evidence for net electron-transfer quenching and to obtain rate constants for back electron transfer. Different spectra taken before and after the flash clearly show the appearance of the expected redox intermediates following either oxidative or reductive quenching.[21] Following flash photolysis, well-defined decay of the redox transients was observed that followed second-order, equal-concentration kinetics in that plots of $1/\Delta A_\lambda$ vs. t, where A_λ is the absorbance change at a wavelength λ, were linear for at least 2–3 half lives. The kinetics and difference spectra observed were consistent in all cases with the observation of back electron transfer following electron-transfer quenching either oxidatively (eq 2) or reductively (eq 3). Rate constants were calculated from

$$Os(phen)_3^{2+*} + p\text{-}Me^+NC_5H_4C(O)NH_2 \rightarrow Os(phen)_3^{3+} + p\text{-}MeNC_5H_4C(O)NH_2 \quad (2)$$

$$Os(phen)_3^{2+*} + p\text{-}Me_2NC_6H_4OMe \rightarrow Os(phen)_3^{+} + p\text{-}Me_2NC_6H_4OMe^+ \quad (3)$$

the slopes of plots of $1/\Delta A_\lambda$ vs. t where slope $= k_b/\Delta\epsilon_\lambda b$. The molar extinction coefficient changes at a given wavelength ($\Delta\epsilon_\lambda$) were determined from the spectra of the components in the reaction. Spectra for the redox transients were generated by electrochemical oxidation or reduction. The rate constant data are summarized in Table III.

Estimation of Excited-State Reduction Potentials. In earlier work it was suggested that excited-state reduction potentials could be estimated on the basis of an analysis of a kinetic quenching scheme first proposed by Rehm and Weller[19,22,23] and shown in Scheme I with the quenching of $Os(phen)_3^{2+*}$ by PQ^{2+} (p-$Me^+NC_5H_4C_5H_4N^+Me$) used as the example. Some of the steps in the scheme are (i) diffusion together of the excited state and quencher followed by electron-transfer quenching, (ii) back electron transfer to re-form the excited state, (iii) back electron transfer giving the ground state of the metal complex, and (iv) diffusional separation of the redox products created by electron-transfer quenching.

Scheme I

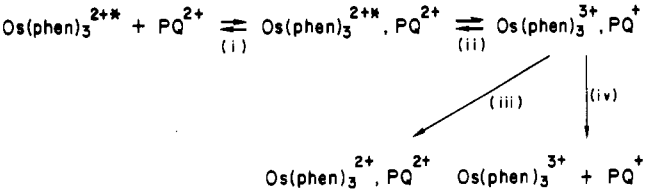

In the limit that re-formation of the excited state (ii) is slow compared to steps iii and iv, it is possible to relate the experimentally observed quenching rate constants to the free energy for the quenching reaction, ΔG_Q, as shown in eq 4.[19] In eq 4, k_q'

$$RT \ln k_q' = RT \ln k_q'(0) - (\Delta G^\circ_Q/2)[1 + \Delta G^\circ_Q/2\lambda] \quad (4)$$

is the quenching rate constant corrected for diffusional effects, $k_q'(0)$ is the quenching rate constant for the case where $\Delta G^\circ_Q = 0$ and λ is 4 times the classical vibrational trapping energy arising from intramolecular and solvent vibrations. Corrections for diffusional effects were made in the usual way on the basis of the equation $1/k_q = 1/k_q' + 1/k_D$.[24,25] Values for the diffusion-limited rate constant, k_D, were calculated from the Debye–Smolchowski equation and reasonable estimates for molecular dimensions. The details of the calculations are available elsewhere.[21]

In the limit that $\Delta G^\circ_Q << 2\lambda$, eq 4 can be simplified, giving eq 5.[19] Using the appropriate relationships between ΔG°_Q and reduction potentials for the excited-state ($E^\circ(Os^{II*/I})$, E°-

$$RT \ln k_q' = RT \ln k_q'(0) - \Delta G^\circ_Q/2 \quad (5)$$

(21) Dressick, W. J. Ph.D. Dissertation, The University of North Carolina, Chapel Hill, NC, 1981.
(22) (a) Rehm, D.; Weller, A. *Ber. Bunsenges. Phys. Chem.* **1969**, *73*, 834. (b) Rehm, D.; Weller, A. *Isr. J. Chem.* **1970**, *8*, 259.
(23) (a) Ballardini, R.; Varani, G.; Indelli, M. T.; Scandola, F.; Balzani, V. *J. Am. Chem. Soc.* **1978**, *100*, 7219. (b) Bock, C. R.; Connor, J. A.; Gutierrez, A. R.; Meyer, T. J.; Whitten, D. G.; Sullivan, B. P.; Nagle, J. K. *Chem. Phys. Lett.* **1979**, *61*, 522.
(24) Noyes, R. M. *Prog. React. Kinet.* **1961**, *1*, 129.
(25) (a) von Smoluchowski, M. *Z. Phys. Chem., Stoechiom. Verwandtschaftsl.* **1917**, *92*, 129. (b) Debye, P. *Trans. Electrochem. Soc.* **1942**, *82*, 265.

Table III. Rate Constant Data for Back Electron Transfer in 0.1 M $LiClO_4$–CH_3CN at 22 ± 2 °C

compd	quencher	reacn[a]	k_b, M^{-1} s^{-1}	λ,[b] nm	$\Delta\epsilon_\lambda$[c]
$(bpy)_2Os(dppm)^{2+}$	PQ^{2+}	$Os^{III} + PQ^+ \rightarrow Os^{II} + PQ^{2+}$	$(2.10 \pm 0.08) \times 10^9$	605	10800
			$(2.31 \pm 0.15) \times 10^9$	397	21200
$(bpy)_2Os(dppm)^{2+}$	10-Me-PTZ	$Os^{I} + 10\text{-Me-PTZ}^+ \rightarrow Os^{II} + 10\text{-Me-PTZ}$	$(5.57 \pm 0.16) \times 10^9$	517	12387
$(phen)_2Os(Me_2PPh)_2^{2+}$	PTZ	$Os^{I} + PTZ^+ \rightarrow Os^{II} + PTZ$[d]	$(1.39 \pm 0.12) \times 10^9$	735	2410
$(phen)_2Os(Me_2PPh)_2^{2+}$	PQ^{2+}	$Os^{III} + PQ^+ \rightarrow Os^{II} + PQ^{2+}$[d]	$(1.25 \pm 0.14) \times 10^{10}$	605	10195
$(trpy)(dppene)Os(py)^{2+}$	PQ^{2+}	$Os^{III} + PQ^+ \rightarrow Os^{II} + PQ^{2+}$	$(5.91 \pm 0.40) \times 10^9$	605	10600
$Os(trpy)_2^{2+}$	PQ^{2+}	$Os^{III} + PQ^+ \rightarrow Os^{II} + PQ^{2+}$	$(1.07 \pm 0.06) \times 10^{10}$	605	9720
$(bpy)Os(das)_2^{2+}$	TBTPA[e]	$Os^{I} + TBTPA^+ \rightarrow Os^{II} + TBTPA$	$(2.50 \pm 0.25) \times 10^8$	703	24700
$(bpy)Os(das)_2^{2+}$	TBTPA, O_2	$O_2^- + TBTPA^+ \rightarrow O_2 + TBTPA$[f]	$(2.65 \pm 0.30) \times 10^8$	703	24700

[a] The reaction is that observed following flash photolysis. The solutions were Ar-bubble deaerated. [b] Wavelength used to monitor the reaction. [c] Extinction coefficient change for the reaction in M^{-1} cm^{-1} at the monitoring wavelength. [d] 0.5 M $LiClO_4$–MeCN. Ar-bubble degassed. [e] TBTPA is $N(p\text{-}C_6H_4Br)_3$. [f] In an aerated solution.

Table IV. Excited- and Ground-State Potentials in Acetonitrile[a]

no.	complex[a]	E_{em} (0–0),[b] V	$E_{1/2}$ ($Os^{III/II}$), V	$E^{\circ\prime}$ ($Os^{III/II*}$),[c] V	$E^{\circ\prime}$ ($Os^{III/II*}$),[d] V	$E_{1/2}$ ($Os^{II/I}$)	$E^{\circ\prime}$ ($Os^{II*/I}$),[e] V	$E^{\circ\prime}$ ($Os^{II*/I}$),[f] V
1	$Os(trpy)_2^{2+}$	1.80	0.97	−0.83		−1.25	0.55	0.60 (±0.10)
2	$(trpy)(dppene)OsCl^+$	(1.83)	0.97	−0.86		−1.20	0.63	0.60 (±0.10)
3	$Os(phen)_3^{2+}$	1.80	0.82	−0.98	−1.06 ± 0.10	−1.21	0.59	0.50 (±0.10)
4	$(phen)_2Os(MeCN)_2^{2+}$	1.91	0.87	−1.04	−0.95 ± 0.10	−1.36	0.55	0.55 (±0.10)
5	$(phen)_2Os(Me_2PPh)_2^{2+}$	2.03	1.09	−0.94	−0.90 ± 0.10	−1.28	0.75	0.68 (±0.10)
6	$(bpy)_2Os(dppm)^{2+}$	(2.10)	1.27	−0.83	−0.90 ± 0.10	−1.26	0.84	0.75 (±0.10)
7	$(phen)_2Os(dppm)^{2+}$	2.13	1.32	−0.81	−0.85 ± 0.10	−1.24	0.89	0.90 (±0.10)
8	$(phen)_2Os(dppene)^{2+}$	2.18	1.36	−0.83	−0.93 ± 0.10	−1.22	0.96	0.95 (±0.15)
9	$(bpy)Os(das)_2^{2+}$	(2.30)	1.48	−0.82	−0.75 ± 0.10	−1.12	1.18	1.08 (±0.10)
10	$(bpy)_2Os(Me_2SO)_2^{2+}$	2.33	1.72	−0.61	−0.70 ± 0.10	−1.20	1.10	1.20 (±0.10)
11	$(bpy)Os(dppene)_2^{2+}$	(2.54)	1.84	−0.70	−0.66 ± 0.10	−1.16	1.38	
12	$(3,4,7,8\text{-}Me_4phen)_2Os(dppene)^{2+}$	(2.23)	1.25	−0.98	−1.05 ± 0.10	−1.51	0.72	
13	$Ru(bpy)_3^{2+}$	2.12	1.29	−0.83	−0.81 ± 0.07	−1.33	0.79	0.77 (±0.07)

[a] At 22 ± 2 °C, I = 0.1 M ($[NEt_4]ClO_4$), vs. the saturated calomel electrode. Note the ligand abbreviations in Table II. [b] Energy of $v' = 0 \rightarrow v = 0$ transition in the emission spectrum for the complex in 4:1 EtOH–MeOH glass at 77 K.[29] [c] Calculated from $E_{em}(0\text{–}0)$ and $E_{1/2}(Os^{III/II})$ using eq 8; the estimated error is ±0.04 V. [d] Estimated from the oxidative quenching data in the supplementary tables. [e] Calculated from $E_{em}(0\text{–}0)$ and $E_{1/2}(Os^{II/I})$ using eq 9; the estimated error is ±0.04 V. [f] Estimated from the reductive quenching data in the supplementary tables.

($Os^{III/II*}$)) and quencher ($E^\circ(Q^{ox/red})$) couples gives eq 6 for reductive quenching and eq 7 for oxidative quenching.[19] In eq

reductive quenching

$$RT \ln k_q' = RT \ln k_q'(0) + \tfrac{1}{2}[E^{\circ\prime}(Os^{II*/I}) - E^{\circ\prime}(Q^{ox/red}) + w_p - w_r] \quad (6)$$

oxidative quenching

$$RT \ln k_q' = RT \ln k_q'(0) - \tfrac{1}{2}[E^{\circ\prime}(Os^{III/II*}) - E^{\circ\prime}(Q^{ox/red}) + w_p - w_r] \quad (7)$$

6 and 7, w_p and w_r are the electrostatic energies associated with bringing together the excited state and quencher and the redox products following quenching, respectively. In acetonitrile solution at room temperature, the electrostatic energies are given approximately by w (V) = $[(0.022)Z_AZ_Bd] \exp[-9/(1 + 0.48dI)^{1/2}]$; d is the interreactant separation in Å, Z_A and Z_B are the charges on the reactants, and I is the ionic strength. Under our conditions, the w terms are small (<0.1 V).

If quenching rate constants are available for a series of related quenchers, it is possible to use eq 6 and 7 to estimate excited-state potentials. The term $k_q'(0)$ is related to the self-exchange rate constants for the excited-state (k_{ES}) and quencher (k_Q) couples by $k_q'(0) = (k_{ES}k_Q)^{1/2}$ if corrections for diffusional effects are included. If k_{ES} and k_Q are known, the hypothetical quencher potential at which $RT \ln k_q'(0) = RT \ln k_q'$ can be evaluated from plots of $RT \ln k_q'$ vs. $E^{\circ\prime}(Q^{+/0})$. At this potential, $\Delta G^{\circ\prime}_Q = 0$, and $E^{\circ\prime}(Os^{II*/I}) = E^{\circ\prime}(Q^{+/0}) + w_r - w_p$ for *reductive quenching* and $E^{\circ\prime}(Os^{III/II*}) = E^{\circ\prime}(Q^{+/0}) + w_p - w_r$ for *oxidative quenching*.[19]

A less precise approach is available if self-exchange rate constant data are not available. If, for such cases, plots of $RT \ln k_q'$ vs. $E^{\circ\prime}(Q^{ox/red})$ show well-defined linear regions with slope = $^1/_2$, i.e. where eq 5 is applicable, the $E^{\circ\prime}(Q^{+/0})$ value at which $\Delta G^{\circ\prime}_Q = 0$ can be estimated as the midpoint of the linear region of the plot where the slope = $^1/_2$. We have used the latter approach to estimate excited-state potentials for the Os complexes. Some representative plots are shown in Figure 2. The linear regions with slope = $^1/_2$ are illustrated with the lines shown, and the approximate midpoints are indicated. The potentials derived from the plots are summarized in Table IV. Since it was not always clear where the lower limit of the linear region ended because of insufficient data, the values cited serve as lower limit estimates of the oxidizing or reducing strengths of the excited states. The kinetic quenching technique is not an extremely accurate method of determining the excited-state potentials since typical error limits

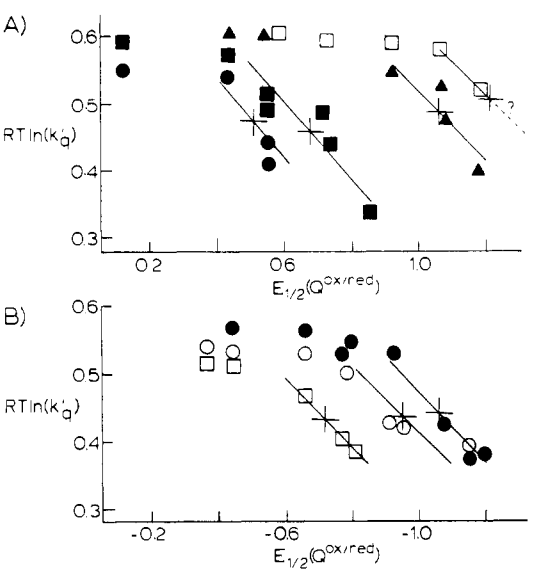

Figure 2. Representative plots of quenching data for (A) reductive quenchers and (B) oxidative quenchers. Drawn lines indicate regions where the slope is $^1/_2$, with the midpoints marked with crosses. Complexes are labeled as follows: ●, $Os(phen)_3^{2+}$; ■, $Os(phen)_2(Me_2PPh)_2^{2+}$; ▲, Os $(bpy)(das)_2^{2+}$, □, Os $(bpy)_2(Me_2SO)_2^{2+}$; ○, $Os(phen)_2(dppene)^{2+}$. Data were taken from Supplementary Tables III and IV.

Table V. Ground- and Excited-State Properties for the Complexes (phen)$Os^{II}L_4^{2+}$ in Acetonitrile[a]

complex	$E_{1/2}$ ($Os^{III/II}$),[b] V	$E_{1/2}$ ($Os^{II/I}$),[b] V	E_{em}, V	E_{em} (0–0),[c] V	τ, ns	ϕ_{em}	$E°$ ($Os^{III/II*}$),[b,d] V	$E°$ ($Os^{II*/I}$),[b,d] V
$(phen)Os(py)_4^{2+}$	0.72	−1.32	1.60	1.69	92	0.0034	−0.97	0.37
$(phen)_2Os(py)_2^{2+}$	0.74	−1.30	1.66	1.72	143	0.0082	−0.98	0.42
$Os(phen)_3^{2+}$	0.82	−1.21	1.72	1.80	262	0.0159	−0.98	0.59
$(phen)_2Os(CH_3CN)_2^{2+}$	0.87	−1.36	1.80	1.91	494	0.0437	−1.04	0.55
$(phen)_2Os(das)^{2+}$	1.11	−1.26	1.86	1.98	608	0.0605	−0.87	0.72
$(phen)_2Os(dppb)^{2+}$	1.23	−1.24	1.96	2.10	1281	0.135	−0.87	0.86
$(phen)_2Os(dpae)^{2+}$	1.28	−1.25	1.99	2.12	1527	0.121	−0.84	0.87
$(phen)_2Os(dppe)^{2+}$	1.30	−1.23	2.00	2.16	1830	0.138	−0.86	0.93
$(phen)_2Os(dppm)^{2+}$	1.32	−1.24	1.99	2.13	1130	0.151	−0.81	0.89
$(phen)_2Os(dppene)^{2+}$	1.36	−1.23	2.04	2.19	1840	0.239	−0.83	0.96
$(phen)Os(das)_2^{2+}$	1.47	−1.25	2.15	2.33	4321	0.361	−0.86	1.08
$(phen)Os(dppene)_2^{2+}$	1.84	−1.25	2.39	2.55	3600	0.518	−0.71	1.30

[a] Data from ref 5, 18, 29. [b] V vs. SSCE in 0.1 M TEAP–CH_3CN solution. [c] $E_{em}(0–0)$ is the 0–0 vibronic energy observed in a 4:1 EtOH–MeOH glass at 77 K. [d] Calculated using eq 8 or 9.

are ±0.10 V. However, the values obtained do clearly illustrate significant variations in values from one complex to another, which was a major goal of the work.

Potentials for the excited-state couples can also be estimated from ground-state reduction potentials and the $v' = 0 \rightarrow v = 0$ emission energy, which is obtainable, at least in principle, from emission spectra. The appropriate relations are given in eq 8 and 9. It should be noted that eq 8 and 9 are only approximate in

$$E°(Os^{III/II*}) = E_{1/2}(Os^{III/II}) - E_{em}(0–0) \quad (8)$$

$$E°(Os^{II*/I}) = E_{1/2}(Os^{II/I}) + E_{em}(0–0) \quad (9)$$

that $E_{em}(0–0)$ includes a contribution from solvent vibrational trapping and is *not* exactly the internal energy difference between the thermally equilibrated ground and excited states. However, the contribution from solvent trapping appears to be relatively small for these complexes.[26]

Reduction of Os(II) to "Os(I)" actually involves the addition of an electron to an orbital that is primarily polypyridine (π^*) in character. Ground-state reduction potentials, $E_{em}(0–0)$ values obtained from emission spectral fits at 77 K in 4:1 v/v ethanol–methanol, and calculated excited-state reduction potentials are also included in Table IV. Because of the difference in media between the $E_{em}(0–0)$ and $E_{1/2}$ values, the values for the excited-state potentials in Table IV are only estimates. Under the circumstances, it is satisfying to note the good agreement obtained by using the two techniques.

Discussion

General Properties. The results presented here establish that facile electron-transfer properties exist for the MLCT excited states of a variety of polypyridyl complexes of Os(II) that differ with regard to both the chromophoric and nonchromophoric ligands. Synthetically, the ligand variations have been accomplished, in the main, by slight variations of routes developed initially by Dwyer and his co-workers.[27] Our results complement those obtained earlier by Crosby et al.[15] and Creutz et al.[12] in using a broadly based series of complexes in which nonchromophoric ligand variations have been extended to include π-acid ligands such as phosphines, arsines, and nitriles.

The Os(II) complexes all exhibit intense absorption bands in the visible region, which are assignable as π^*(polypyridine) ← $d\pi$(metal) MLCT transitions as discussed elsewhere.[15,18,28] The assignments are verified by noting that absorption energy maxima increase linearly with $E_{1/2}(Os^{III/II}) - E_{1/2}(Os^{II/I})$ (Tables I, IV, and V) as expected for MLCT transitions of the type Os^{II}(bpy) → Os^{III}(bpy^{-}·). The emitting excited states are readily assigned as being the converse ligand to metal charge transfer (LMCT) transitions on the basis of the fact that variations in emission energy increase linearly with absorption band energies (Tables I and V) and that they also vary linearly with $E_{1/2}(Os^{III/II}) - E_{1/2}(Os^{II/I})$. The involvement of the ligands in the excited states is also strongly implicated by the appearance of polypyridyl-based, ring-stretching vibrational progressions, which appear with spacings at 1300–1400 cm^{-1} in low-temperature emission spectra.[29b]

The photophysical properties of the polyridyl complexes of Os are closely related to those of analogous complexes of Ru. However, a major difference does exist in terms of photochemical instability toward ligand loss. For $Ru(bpy)_3^{2+}$ and related complexes, thermal population of low-lying old dd states can drastically reduce excited-state lifetimes and lead to decomposition by loss of ligands.[7-11] For related complexes of iron, excited-state properties are dominated by dd states that lie lower than the MLCT states because of the smaller $10Dq$ value of the first-row compared to the second-row transition metals.[30]

On the other hand, the majority of polypyridine complexes of Os that have been investigated so far are remarkably stable photochemically. The photochemical stability is, no doubt, a direct consequence of the still higher $10Dq$ for Os, which raises the energies of low-lying dd states beyond significant thermal population at room temperature. The absence of low-lying dd states is also evidenced by relatively temperature-independent lifetimes for the Os complexes, at least above 200 K. Above 200 K the series of low-lying MLCT states that constitute the "MLCT state" alluded to here reach a sufficient thermal population to behave as a single state.[31]

However, photosubstitution can appear for the Os complexes. Examples include $Os(bpy)_2(Me_2SO)_2^{2+}$,[18] where the high-energy-emitting MLCT state(s) may approach the dd state in energy, and certain trpy complexes of Os where the inability of the trpy ligand to span 180° may cause mixing between the $d\pi$ and $d\sigma^*$ orbitals, lowering the energy of low-lying dd states.[6] It is also possible that photosubstitution could occur from MLCT states containing weak σ-donor ligands, a question that remains to be explored mechanistically.

Quenching Studies. The Os-based excited states undergo facile, net oxidative or reductive quenching as shown by (1) the magnitude of quenching rate constants, (2) the appearance of the

(26) Kober, E. M.; Sullivan, B. P.; Meyer, T. J. *Inorg. Chem.* **1984**, *23*, 2098.
(27) (a) Buckingham, D. A.; Dwyer, F. P.; Goodwin, H. A.; Sargeson, A. M. *Aust. J. Chem.* **1964**, *17*, 325. (b) Buckingham, D. A.; Dwyer, F. P.; Goodwin, H. A.; Sargeson, A. M. *Ibid.* **1964**, *17*, 315. (c) Buckingham, D. A.; Dwyer, F. P.; Sargeson, A. M. *Ibid.* **1964**, *17*, 622.
(28) Bryant, G. M.; Ferguson, J. E.; Powell, H. K. J. *Aust. J. Chem.* **1971**, *24*, 257.
(29) (a) Kober, E. M.; Caspar, J. V.; Sullivan, B. P.; Meyer, T. J., manuscript in preparation. (b) Caspar, J. V. Ph.D. Dissertation, The University of North Carolina, Chapel Hill, NC, 1982. (c) Kober, E. M. Ph.D. Dissertation, The University of North Carolina, Chapel Hill, NC, 1982.
(30) Bergkamp, M. A.; Brunschwig, B. S.; Gutlich, P.; Netzel, T. L.; Sutin, N. *Chem. Phys. Lett.* **1981**, *81*, 147.
(31) (a) Lacky, D. E.; Pankuch, B. J.; Crosby, G. A. *J. Phys. Chem.* **1980**, *84*, 2068. Pankuch, B. J.; Lacky, D. E.; Crosby, G. A. *Ibid.* **1980**, *84*, 2061. (b) Allsopp, S. R.; Cox, A.; Kemp, T. J.; Reed, W. J.; Carassiti, V.; Traverso, O. *J. Chem. Soc., Faraday Trans. 1* **1979**, *79*, 353. (c) Kober, E. M.; Meyer, T. J., submitted for publication.

expected redox products following flash photolysis, and (3) photochromic behavior of solutions containing the Os(II) complexes and oxidative or reductive quenchers. Following the quenching reactions, rapid, back electron transfer reactions occur between either the Os(III) or the ligand-reduced Os(I) complexes and the reduced or oxidized forms of the quencher, showing that the Os complexes are capable of functioning as electron-transfer photocatalysts.

Excited-state redox potentials were evaluated by the kinetic quenching technique as described above. The values obtained from the kinetic quenching technique were found to be in reasonable agreement with values calculated from ground-state reduction potentials and the internal energy differences between the excited and ground states calculated from the approximation $|\Delta E| \sim E_{em}(0\text{–}0)$ (Table IV).

It is illustrative to compare the results obtained here using the kinetic quenching technique with results obtained earlier. For the excited-state couples involving $Ru(bpy)_3^{2+*}$, estimates of self-exchange rate constants give a value of 0.52 V as the potential at which $RT \ln k_q' = RT \ln k_q'(0)$ (note eq 6 and 7) for both oxidative and reductive quenching.[19] The midpoints calculated with the technique described here and from the same data are found at $RT \ln k_q' = 0.48 \pm 0.02$ V for reductive quenching and 0.45 ± 0.03 V for oxidative quenching of $Ru(bpy)_3^{2+*}$. The origin of the discrepancy is unclear, but the differences are well within the stated uncertainty of ±0.1 V.

An important point arises from the collection of excited-state redox potentials in Figure 2 and Table IV. From the data it can be seen that the changes made in the nonchromophoric ligands lead to variations in redox potentials for the excited states as oxidants ($E°(Os^{II*/I})$) that span a range of 0.8 V. These synthetically derived changes give a series of excited states that range in potential from $Os(phen)_3^{2+*}$, which is a somewhat mild oxidizing agent ($E°' = 0.59$ V), to $Os(bpy)(dppene)_2^{2+*}$, which is impressive for its strength as an oxidant ($E°' = 1.38$ V). Variations in redox potentials for the excited states acting as reducing agents, $E°(Os^{III/II*})$, are less impressive but span a range of 0.4 V. Given the potentials, all of the excited states are capable of functioning as weak to moderate reducing agents ($E°' = -0.6$ to -1.0 V).

Synthetic Control of Excited States. The first theme of this paper was to introduce the kinetic and thermodynamic electron-transfer properties of a series of MLCT excited states of Os(II). Inspection of the data in Table IV shows that clear trends exist between such excited-state properties as redox potentials and emission energies and the ground-state properties $E_{1/2}(Os^{III/II})$ and $E_{1/2}(Os^{II/I})$. In that the ground-state redox potentials vary systematically as the ligands are varied, the possibility exists that ligand variations can be used to vary excited-state properties in a systematic way. It is even conceivable that the implied synthetic control of excited-state properties could be extended beyond emission energies and redox potentials to lifetimes and emission quantum yields. Lifetimes and emission quantum yields are determined by the magnitudes of radiative (k_r) and nonradiative (k_{nr}) rate constants—$\tau = (k_r + k_{nr})^{-1}$, $\phi_{em} = k_r\tau^{-1}$—and for a series of complexes where the metal–ligand basis for the chromophore remains the same, variations in k_r and k_{nr} are determined largely by variations in E_{em}.[1c,5,9,13]

In order to extend such ideas to correlations involving τ and ϕ_{em}, the series of complexes used must be chosen with care: (1) The same pattern of acceptor vibrations, which determine emission band shapes and the Franck–Condon factors for nonradiative decay, must exist throughout. (2) Systems having the same pattern of excited states and excited states having the same orbital and spin origins must be compared. k_r and k_{nr} depend on the electronic nature of the transitions, k_r through the electronic dipole moment inregral and k_{nr} through a vibrationally induced electronic coupling integral. (3) It follows from point 2 that, for correlations involving MLCT states, the metal–ligand chromophoric pair must remain constant through the series.

We have access to such a series in the complexes $(phen)OsL_4^{2+}$ (L = pyridine, CH_3CN, PR_3, AsR_3, ...) where systematic variations

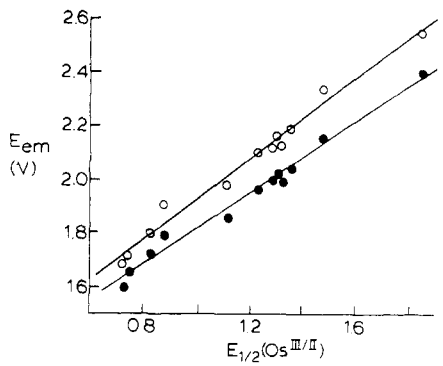

Figure 3. Dependence of emission energy on $E_{1/2}(Os^{III/II})$: bottom curve, E_{em} = emission maximum in room-temperature CH_3CN solution; top curve, $E_{em}(0\text{–}0)$ = emission maximum of $v' = 0$, $v = 0$ vibrational component in 4:1 EtOH–MeOH glass at 77 K. Data were taken from Table V.

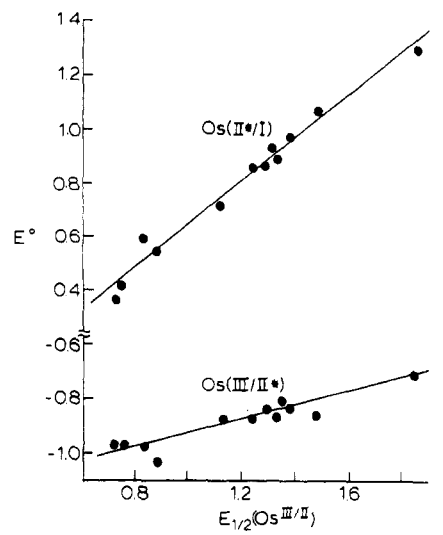

Figure 4. Dependence of the excited-state redox potentials $E°(Os^{III/II*})$ and $E°(Os^{II*/I})$ on $E_{1/2}(Os^{III/II})$. Data were taken from Table V.

are made in the nonchromophoric ligands. Note the data in Table V. The striking fact that emerges from the data is that variations in the critical properties that define the excited states—E_{em}, $E°'$, τ, and ϕ_{em}—are paralleled by variations in a single ground-state property, the potential, for the Os(III/II) couple. As a consequence, it is possible to estimate excited-state properties to a reasonable degree of accuracy for the series by a simple ground-state electrochemical measurement.

The point is made graphically by the plots in Figures 3–5. As noted below, the fundamental parameter that dictates excited-state properties is the emission energy, and it is only because variations in $E_{1/2}(Os^{III/II})$ parallel variations in E_{em}, as shown in Figure 3, that the well-defined relationships in Figures 4 and 5 exist.

As shown by the data in Table V and the plots in Figure 4, significant variations in $E_{1/2}(Os^{III/II})$ occur by making what appear to be relatively straightforward variations in the nonchromophoric ligands. The majority of the effect can probably be accounted for, at least qualitatively, by electronic effects, but such arguments neglect variations in solvation energy differences between the +3, Os(III), and +2, Os(II), ions.[32a] In any case, it is expected that stabilization of the $(d\pi)^5Os(III)$ ion will be enhanced by σ- and/or π-donor ligands. Enhanced stabilization of $(d\pi)^6Os(II)$ is expected to occur for good back-bonding ligands.[32b] Back-bonding stabilization of Os(II) may be the more important effect, as evidenced, for example, by the increase in $E_{1/2}(Os^{III/II})$ when polypyridyl ligands are replaced by arylphosphines. An XPS study

(32) (a) Buckingham, D. A.; Sargeson, A. M. "Chelating Agents and Metal Chelates"; Dwyer, F. P., Mellor, D. P., Eds.; Academic Press: New York, 1964. (b) Taube, H. *Surv. Prog. Chem.* **1973**, *6*, 1.

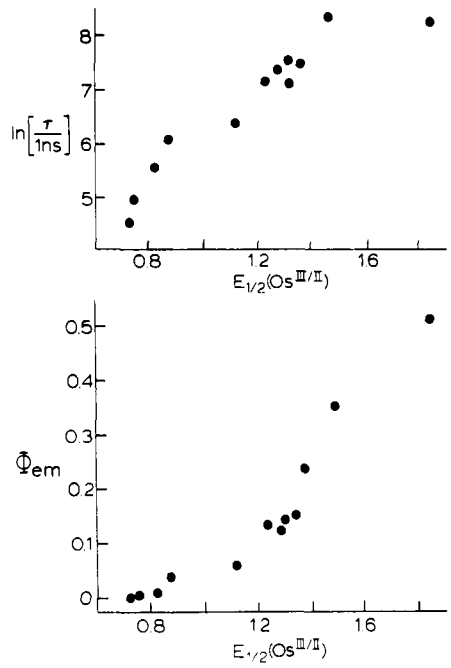

Figure 5. Dependence of excited-state lifetime (τ) and quantum yield for emission (ϕ_{em}) upon $E_{1/2}(Os^{III/II})$. Data were taken from Table V.

has shown that such variations lead to an enhanced electron deficiency at Ru(II).[33]

In contrast to $E_{1/2}(Os^{III/II})$, the phen-based $Os^{II/I}$ couples are only slightly dependent on variations in the nonchromophoric ligands. (As an aside, the slight variations in the $Os^{II/I}$ couple with L show that variations in solvation energy terms can not play an important role in determining the variations observed for the $Os^{III/II}$ couples.) Significant variations in $E_{1/2}(Os^{II/I})$ are not expected because the acceptor orbital is largely π^*(phen) in character. Some variation does exist because of $d\pi-\pi^*$(phen) mixing with Os(II).[29c] The small variations can be explained in the following way: (1) As the Os(II) center becomes more difficult to oxidize, the energy of the $d\pi$ orbitals is lowered relative to that of the free electron in a vacuum. (2) A relative stabilization of the $d\pi$ levels also leads to a stabilization of the π^*(phen) orbitals because of a decrease in $d\pi-\pi^*$(phen) mixing, which depends on the energy gap between them. (3) As the extent of mixing decreases and the π^*(phen) orbitals become more purely ligand in character, the π^*(phen) orbitals become better electron acceptors.

Emission Energy. When the discussion above and the nature of the emission process are considered, $(phen^{-}\cdot)Os^{III}L_4^{2+} \rightarrow (phen)Os^{II}L_4^{2+}$, it is not surprising that linear correlations exist between $E_{1/2}(Os^{III/II})$ and both E_{em}, the emission energy in acetonitrile solution at room temperature, and $E_{em}(0\text{–}0)$, the emission maximum for the $v' = 0 \rightarrow v = 0$ vibrational components obtained by spectral fitting of the emission spectra of the complex in a 4:1 ethanol–methanol glass at 77 K. It should be noted that the lowest energy λ_{max} and other features in the absorption spectra show similar linear trends with $E_{1/2}(Os^{III/II})$ as expected.

For $E_{em}(0\text{–}0)$, the slope of the least-squares line (slope = 0.93 ± 0.09) shown in Figure 3 is slightly less than 1. Even though emission, $(phen)Os^{III}L_4^{2+*} \xrightarrow{-h\nu} (phen)Os^{II}L_4^{2+}$, and reduction, $(phen)Os^{III}L_4^{3+} + e^- \rightarrow (phen)Os^{II}L_4^{2+}$, are related processes, the fact that they do not vary identically in the same way with L, which would give a slope of 1, is not surprising. Contributions to a nonunit slope can appear from (1) the fact that $E_{1/2}(Os^{II/I})$ is not constant but shifts slightly with $E_{1/2}(Os^{III/II})$ and (2) the differences in electron–electron repulsion and solvation energy terms between the two types of processes.

For E_{em}, the slope of the line is less (slope = 0.81 ± 0.11). From the results of the spectral-fitting experiments alluded to above, the origin of the decrease in slope appears to be straightforward. At room temperature, the measured emission energy includes contributions both from the internal energy differences between the ground and excited states (ΔE) and from the extent of distortion between ground and excited states both in intramolecular vibrations, x_i, and in surrounding solvent, x_0, $E_{em} = |\Delta E| + x_0 + x_i$ and $E_{em}(0\text{–}0) = |\Delta E| + x_0$. The extent of distortion and therefore the magnitude of the contributions from x_0 and x_i depend on the *extent* of charge transfer between the ground and excited states. As $|\Delta E|$ increases, the extent of $d\pi-\pi^*$(phen) mixing decreases, the extent of charge transfer increases, and both x_0 and x_i increase in magnitude. The effects of enhanced vibrational distortion include a broadening of the emission manifold and a shifting of E_{em}, measured as the position of maximum emission intensity, to energies increasingly lower than ΔE as $|\Delta E|$ increases.[29b]

Excited-State Redox Potentials. With the linear relationship between E_{em} and $E_{1/2}(Os^{III/II})$ established (Figure 3), it follows immediately from eq 8 and 9 that excited-state redox potentials for the couples $Os^{II*/I}$ and $Os^{III/II*}$ should vary with $E_{1/2}(Os^{III/II})$. That such is the case is shown in Figure 4. From these data, the potential for the excited state acting as an oxidant, $E_{1/2}(Os^{II*/I})$, is strongly dependent upon $E_{1/2}(Os^{III/II})$ (slope = 0.79 ± 0.10). The dependence is to be expected since, in essence, both processes involve the reduction of Os(III) to Os(II), $(phen^{-}\cdot)Os^{III}L_4^{2+*} + e^- \rightarrow (phen^{-}\cdot)Os^{II}L_4^{+}$ and $(phen)Os^{III}L_4^{3+} + e^- \rightarrow (phen)Os^{II}L_4^{2+}$. The consistently lower values (0.4–0.5 V) for the excited-state couples show that the excited states are less powerful oxidants than the corresponding Os(III) complexes. The bases for the decrease are as follows: (1) Reduction of the Os^{III} ground state necessarily involves an oxidant of higher charge (3+/2+ vs. 2+/1+ for the excited state) and in the context of an appropriate thermodynamic cycle is favored electrostatically in both the solvation and the ionization energy terms. (2) For the excited state, the Os(III) ion is bound to a phen radical anion as ligand. The ligating properties of the reduced ligand are expected to be altered significantly compared to those of 1,10-phenanthroline. In particular, upon reduction, the abilities of the ligand as both a σ and a π donor should be greatly enhanced. As a consequence, the Os^{III} stie in the excited state is within a more electron-rich environment and is expected to be less electron deficient.

From the data in the same figure for the $Os^{III/II*}$ couples, it is obvious that the ability of the excited states to act as reductants depend only weakly on $E_{1/2}(Os^{III/II})$. This is not surprising since the excited-state couple involves a ligand-localized reduction, $(phen)Os^{III}L_4^{3+} + e^- \rightarrow (phen^{-}\cdot)Os^{III}L_4^{2+*}$ and the situation is much the same as for the $Os^{II/I}$ ground-state couple, $(phen)Os^{II}L_4^{2+} + e^- \rightarrow (phen^{-}\cdot)Os^{II}L_2^{+}$. The excited states are weaker as reducing agents than the reduced ground-state complexes by 0.4–0.5 V. As for the comparison involving the excited states as oxidants, this is an expected result for the following reasons: (1) The excited-state couple involves 3+ and 2+ ions compared to 2+ and 1+ ions for the ground-state couple. In the context of an appropriate thermodynamic cycle, loss of an electron from the 2+ excited state is more difficult than from the 1+ reduced ground state on electrostatic grounds. (2) For the reduced ground-state couple, the added electron is in a phen ligand that is coordinated to a $(d\pi)^6$Os(II) ion and Os(II) is a relatively good $d\pi$ donor. The effect of $d\pi-\pi^*$(phen) mixing is to destabilize the π^*(phen) orbitals, leading to stronger reducing properties. In the excited state, the $(d\pi)^5$Os(III) site is expected to be a much weaker π donor and probably a reasonable π acceptor, leaving the π^*(phen) levels more purely ligand in character.

Once again, it is worth noting the rather profound changes that can be wrought in excited- and ground-state redox potentials by relatively simple variations in the nonchromophoric ligands. In particular, for the ground- and excited-state couples as oxidants, the range in potentials for the $Os^{III/II}$ couples is 1.1 V and for the excited-state $Os^{II*/I}$ couples it is 0.9 V. These rather extended ranges are in contrast to the narrow ranges for the $Os^{II/I}$ and $Os^{III/II*}$ couples.

Lifetime and Emission Quantum Yields. The magnitudes of excited-state lifetimes (τ) and emission quantum yields (ϕ_{em}) are

(33) Connor, J. A.; Meyer, T. J.; Sullivan, B. P. *Inorg. Chem.* **1979**, *18*, 1388.

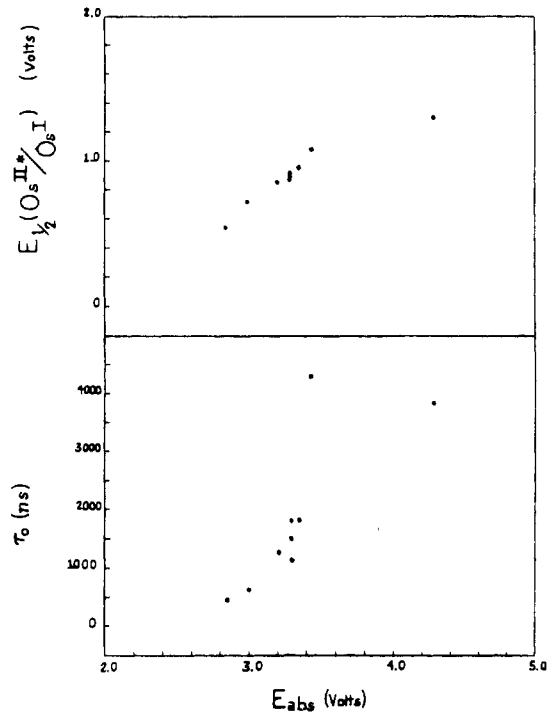

Figure 6. Variations of τ and $E_{1/2}(Os^{II*/I})$, the redox potential for the excited-stte acting as oxidant, with E_{abs}, the energy of maximum absorptivity in the low-energy-absorption spectrum. The data are for the last nine entries in Table V for which there are single, well-defined absorption maxima.

determined by the rate constants for radiative (k_r) and nonradiative (k_{nr}) processes as shown in eq 10 and 11. We have shown that

$$1/\tau = k_r + k_{nr} \tag{10}$$

$$\phi_{em} = k_r/(k_r + k_{nr}) \tag{11}$$

nonradiative decay in Os^{II}–polypyridine MLCT excited states can be well described by using the low-temperature, weak vibrational coupling limit of radiationless decay theory.[5,9,34] In this limit, if the electronic basis for the chromophore and the nature of the deactivating or acceptor vibrations remain the same through a series of excited states, k_{nr} is predicted to vary with $E_{em}(0-0)$ as shown in eq 12.[34] In eq. 12, A and B are constants, positive in

$$\ln k_{nr} \approx A - BE_{em} \tag{12}$$

value, that depend upon the magnitude of the vibrationally induced electronic coupling between states and the properties of the acceptor vibrations, respectively.

By the same token, k_r is predicted to vary as E_{em}^3 as shown in eq 13 and as predicted by the Einstein coefficient for spontaneous emission.[35] C is a positive constant that includes the transition moment integral squared.

$$k_r \approx CE_{em}^3 \tag{13}$$

Two points emerge from the plots of ln τ and ϕ_{em} vs. $E_{1/2}(Os^{III/II})$ in Figure 5. The first is that realistic estimates for τ and ϕ_{em} for an as yet unmeasured complex of the type (phen)OsL_4^{2+} can be made once $E_{1/2}(Os^{III/II})$ is known. The values are available by using the data in Figure 6 to estimate the excited-state quantities. However, once again, note that such predictions are only possible for compounds in a series where (1) the chromophoric basis, in this case metal plus ligand, remains the same, (2) the pattern of vibrations that dominate nonradiative decay is a constant, (3) the medium is the same, and (4) there are no additional low-lying states that influence τ or ϕ_{em} as is the case for the low-lying dd states in the series $Ru(bpy)_2(L)_2^{2+}$.[9a]

A second point to emerge from Figure 5 is that the variations in ln τ and ϕ_{em} are understandable in terms of eq 12 and 13. The key is that k_{nr} *decreases* exponentially with E_{em} or $E_{1/2}(Os^{III/II})$ while k_r *increases* as the cube of E_{em}. For compounds with low excited-state energies (E_{em} = 1.6–2.1 V), $k_{nr} >> k_r$. For these excited states, $\tau = k_r^{-1} + k_{nr}^{-1} \sim k_{nr}^{-1}$ and $\phi_{em} << 1$. It follows, for these excited states, that $\tau = k_{nr}^{-1}$, and since ln $k_{nr} \propto E_{1/2}(Os^{III/II})$, the linear region in the plot of ln τ vs. $E_{1/2}(Os^{III/II})$ can be explained.

As E_{em} increases and k_{nr} decreases, k_r becomes competitive with k_{nr}. In this limit the variation of ϕ_{em} with E_{em} or $E_{1/2}(Os^{III/II})$ becomes complex. In the limit of high E_{em}, $k_r \sim k_{nr}$, ϕ_{em} approaches 1, and τ, instead of *decreasing* exponentially, begins to *increase*.

In terms of changes in electronic structure induced by ligand variations, further increases in MLCT excited-state energy to the region where $k_r > k_{nr}$ are probably somewhat limited experimentally. With further increases in energy, the MLCT excited states would lie above ligand-based $^3(\pi-\pi^*)$ states as signalled by a fundamental change in the properties of the excited-state emission.[36]

Conclusions. A number of useful conclusions emerge from this work that relate in a fundamental way to the design of MLCT chromophores and excited states: (1) Polypyridyl complexes of Os(II) provide a basis for a series of MLCT excited states that undergo facile oxidative and reductive quenching. (2) Compared to related complexes of Ru(II), the Os complexes offer the advantage of photostability. The origin of the photostability is in the absence of low-lying dd states. For the Os complexes, the higher $10Dq$ value for Os(II) compared to Ru(II) increases the energies of low-lying dd states to the point where they are no longer appreciably populated at room temperature. (3) In the series $(phen)OsL_4^{2+}$, variations in the nonchromophoric ligands L lead to systematic changes in E_{em}, k_r, k_{nr}, τ, ϕ_{em}, and excited-state redox potentials for the emitting ^{3}MLCT states. (4) Remarkably, but in retrospect understandably, the variations in excited-state properties correlate well with $E_{1/2}(Os^{III/II})$ for the ground state. (5) Because of the systematic variations with L and the flexibility of the background synthetic chemistry, it is possible to design complexes with predictable excited-state properties. (6) Within a series of related excited states like $(phen)OsL_4^{2+*}$, the choice of desirable properties as a potential redox photosensitizer is dependent upon three key properties: ground-state absorption, excited-state redox potentials, and excited-state lifetime. Figure 6 shows excited-state lifetimes and redox potentials for the excited states acting as oxidant [$(E_{1/2}(Os^{II*/I})$] plotted against the energy of the position of maximum absorptivity in the low-energy-absorption manifold (E_{abs}). The complexes are all broad-band absorbers in the visible and near UV regions, and the E_{abs} values are a relative measure of light absorptivity ability in the visible region. The plots are based on the last nine entries in Table V, where there are single, well-defined low-energy absorption maxima. Recall that variations in E_{abs} are paralleled by variations in E_{em}. The data in Figure 6 illustrate the sometimes contradictory results that variations in the nonchromophoric ligands can have in terms of desirable properties as a sensitizer. In particular, the figure shows that there is a gain in excited-state redox potential and lifetimes as E_{abs} increases but that the gain is at the expense of a decreased absorptivity in the visible region of the spectrum. (7) The variations explored here have been based on changes in the nonchromophoric ligands. Within the broad, general class of compounds containing low-lying MLCT excited states it is also possible to explore variations based on the metal (Ir^{III}, Ru^{II}, Os^{II}, Re^{I}, Mo^0) and/or variations based on the chromophoric poly-

(34) (a) Freed, K. F.; Jortner, J. *J. Chem. Phys.* **1970**, *50*, 6272. (b) Englman, R.; Jortner, J. *Mol. Phys.* **1970**, *18*, 145. (c) Lin, S. H. *J. Chem. Phys.* **1966**, *44*, 3759.

(35) (a) Herzberg, G. "Molecular Spectra and Molecular Structure", 2nd. ed.; Van Nostrand: Princeton, NJ, 1950; Vol. 1, Chapter 4. (b) Ballhausen, C. J. "Molecular Electronic Structures of Transition Metal Complexes"; McGraw-Hill: New York, 1978.

(36) Belser, P.; Von Zelewsky, A.; Juris, A.; Barigelletti, F.; Tucci, A.; Balzani, V. *Chem. Phys. Lett.* **1982**, *89*, 101.

pyridyl ligand. Such variations necessarily lead to perturbations in the basic chromophore but offer some obvious advantages. One, in particular, in terms of excited-state redox potentials, is the possibility of manipulating potentials of the excited states as reductants, by varying the π^* levels of the chromophoric ligand. Such variations will be the subject of a forthcoming publication.[37]

Acknowledgment is made to the Department of Energy under Grant No. DE-AS05-78EE06034 for support of this research.

Registry No. **1**, 85452-91-1; **2**, 79968-44-8; **3**, 31067-98-8; **4**, 80502-77-8; **5**, 80558-59-4; **6**, 75441-72-4; **7**, 75446-24-1; **8**, 75446-26-3; **9**, 96964-76-0; **10**, 80502-69-8; **11**, 89711-31-9; **12**, 96964-77-1; **13**, 15158-62-0; $(phen)Os(py)_4^{2+}$, 80502-71-2; $(phen)_2Os(py)_2^{2+}$, 80502-73-4; $(phen)_2Os(das)^{2+}$, 96964-78-2; $(phen)_2Os(dppb)^{2+}$, 96964-79-3; $(phen)_2Os(dpae)^{2+}$, 80502-85-8; $(phen)_2Os(dppe)^{2+}$, 80502-83-6; $(phen)Os(das)_2^{2+}$, 80502-87-0; $(phen)Os(dppene)_2^{2+}$, 96964-80-6; BZQ^{2+}, 13096-46-3; PQ^{2+}, 4685-14-7; $Mepy\text{-}4CN^+$, 13441-45-7; $Mepy\text{-}4CO_2Me^+$, 38117-49-6; $Etpy\text{-}4CO_2Me^+$, 48128-20-7; $Etpy\text{-}4CONH_2^+$, 71258-88-3; $Mepy\text{-}4CONH_2^+$, 45791-94-4; $Bzpy\text{-}3CONH_2^+$, 16183-83-8; $Etpy\text{-}3CONH_2^+$, 71413-64-4; $Mepy\text{-}3CONH_2^+$, 3106-60-3; TMPD, 100-22-1; TMBD, 366-29-0; 3-MeO-PTZ, 1771-19-3; PTZ, 92-84-2; 4-MeO-DMA, 701-56-4; 2-Cl-PTZ, 92-39-7; $2\text{-}CF_3$-PTZ, 92-30-8; 4-Me-DMA, 99-97-8; 10-Me-PTZ, 1207-72-3; DMA, 121-69-7; 4-Br-DMA, 586-77-6; TPA, 603-34-9; TBTPA, 4316-58-9; PXT, 262-20-4.

Supplementary Material Available: Tables of redox potentials for 10 oxidative quenchers and 14 reductive quenchers and tables of oxidative and reductive quenching rate constants for a series of Os(II) MLCT excited states (4 pages). Ordering information is given on any current masthead page.

(37) Johnson, S.; Westmoreland, T. D.; Kober, E. M.; Sullivan, B. P.; Caspar, J. V.; Meyer, T. J., manuscript in preparation.

Contribution from the Departments of Chemistry, University of Santa Clara, Santa Clara, California 95053, and University of Colorado, Boulder, Colorado 80309

First-Row Transition-Metal Complexes of Pyridine-2,6-dicarboxylic Acid *N*-Oxide. Crystal Structure of Diaqua(pyridine-2,6-dicarboxylate *N*-oxido)manganese(II)

LAWRENCE C. NATHAN,*† CHRISTINE A. DOYLE,† ANNE M. MOORING,† DONALD C. ZAPIEN,† SCOTT K. LARSEN,‡ and CORTLANDT G. PIERPONT‡

Received July 9, 1984

Five complexes with general formula $M(pdcO)(H_2O)_2$ (where $pdcO^{2-}$ is the pyridine-2,6-dicarboxylate *N*-oxide ion and M^{2+} is Mn, Co, Ni, Cu, and Zn) have been synthesized and characterized by elemental analyses, infrared and electronic absorption spectroscopy, and magnetic susceptibility measurements. The crystal structure of $Mn(C_7H_3NO_5)(H_2O)_2$ was determined. The complex is polymeric with manganese six-coordinated to two bridging *N*-oxide groups (trans), two terminal carboxyl groups (cis), and two water molecules (cis). Crystal data: orthorhombic, space group *Pcca*, $a = 8.005$ (1) Å, $b = 6.334$ (2) Å, $c = 18.673$ (4) Å, $Z = 4$, $R = 0.0363$, 1030 reflections. X-ray powder diffraction patterns indicate that all five complexes are not isomorphous.

Introduction

Although the coordinating properties of heterocyclic amine *N*-oxides have been the subject of three review articles,[1-3] the ligand pyridine-2,6-dicarboxylic acid *N*-oxide (hereafter abbreviated as H_2pdcO) has received virtually no attention. This unique ligand was of interest for several reasons. First, its parent amine, pyridine-2,6-dicarboxylic acid (also known as dipicolinic acid), has been thoroughly studied and is known to coordinate unpredictably as the neutral molecule, the univalent anion, or the divalent anion, bidentate in some cases and tridentate in others.[4-7] Second, while essentially all reported *N*-oxide complexes are neutral or cationic,[1-3] H_2pdcO may form anionic *N*-oxide complexes. Third, H_2pdcO may form binuclear or polymeric complexes with first-row transition-metal ions. We are aware of only one report of a complex of H_2pdcO, namely $UO_2(pdcO)\cdot 3H_2O$, which is dimeric with tridentate $pdcO^{2-}$ ligands in which the *N*-oxide oxygen and one carbonyl group coordinate to one uranium while the remaining carboxyl group is coordinated to the second uranium.[8]

Experimental Section

Synthesis of Pyridine-2,6-dicarboxylic Acid *N*-Oxide, $C_7H_5NO_5$ (H_2pdcO). The ligand H_2pdcO was prepared in 66% yield by hydrogen peroxide oxidation of the parent amine by the method of Syper and co-workers.[9] The extraction step was done with a continuous liquid extractor. Mp: 157-159 °C (lit.[9] mp 158-160 °C).

Synthesis of the Complexes. A 25-mL aliquot of a hot aqueous solution containing 5 mmol of pyridine-2,6-dicarboxylic acid *N*-oxide was added with stirring to 25 mL of hot aqueous solution containing 5 mmol of the appropriate hydrated metal acetate, $M(C_2H_3O_2)_2\cdot nH_2O$ (M = Mn, Co, Ni, and Cu and $n = 4$; M = Zn and $n = 2$). Except for the manganese complex, the product precipitated almost immediately. The manganese complex was obtained by reducing the volume of water and allowing the solution to cool overnight. The products were filtered, washed with small portions of cold water, and dried under vacuum over phosphorus pentoxide. Yields of the $M(pdcO)(H_2O)_2$ complexes ranged from 70 to 100%. $MnC_7H_7O_7N$: yellow; dec pt 257-263 °C. Anal. Calcd: C, 30.90; H, 2.59; N, 5.15. Found: C, 30.94; H, 2.72; N, 5.07. $CoC_7H_7O_7N$: pink; dec pt 235-238 °C. Anal. Calcd: C, 30.45; H, 2.56; N, 5.07. Found: C, 30.25; H, 2.70; N, 4.95. $NiC_7H_7O_7N$: green; dec pt 265-270 °C. Anal. Calcd: C, 30.48; H, 2.56; N, 5.08. Found: C, 30.54; H, 2.68; N, 5.04. $CuC_7H_7O_7N$: blue; dec pt 268-271 °C. Anal. Calcd: C, 29.95; H, 2.51; N, 4.99. Found: C, 29.75; H, 2.63; N, 4.90. $ZnC_7H_7O_7N$: white; dec pt 240-242 °C. Anal. Calcd: C, 29.76; H, 2.50; N, 4.96. Found: C, 29.62; H, 2.77; N, 4.85.

Physical and Spectral Measurements. Magnetic susceptibility measurements were done on solid samples by the Gouy method at 296-297 K and 5400 G. $HgCo(SCN)_4$ was used as calibrant. Diamagnetic corrections were made by using Pascal's constants. The temperature-independent paramagnetism correction of 60×10^{-6} cgsu was used for the copper complex. The pooled standard deviation from up to five replicate measurements on each compound was 0.05 μ_B. Due to the insolubility of the complexes, electronic absorption spectra were obtained on solid samples as Nujol mulls on Cary 14 and Beckman DBGT spectrophotometers. Infrared spectra were obtained as KBr pellets and as Nujol mulls on a Beckman IR-8 spectrophotometer. X-ray powder diffraction data were obtained by using a Diano XRD-8000 semiauto-

† University of Santa Clara.
‡ University of Colorado.

(1) Orchin, M.; Schmidt, P. J. *Coord. Chem. Rev.* **1968**, *3*, 345.
(2) Garvey, R. G.; Nelson, J. H.; Ragsdale, R. O. *Coord. Chem. Rev.* **1968**, *3*, 375.
(3) Karayannis, N. M.; Pytlewski, L. L.; Mikulski, C. M. *Coord. Chem. Rev.* **1973**, *11*, 93.
(4) Furst, W.; Gouzenh, P.; Jeannin, Y. *J. Coord. Chem.* **1978**, *8*, 237.
(5) Fowles, G. W. A.; Matthews, R. W.; Walton, R. A. *J. Chem. Soc. A* **1968**, 1108.
(6) Chiesi Villa, A.; Guastini, C.; Musatti, A.; Nardelli, M. *Gazz. Chim. Ital.* **1972**, *102*, 226.
(7) Biagini, M.; Chiesi Villa, A.; Guastini, C.; Nardelli, M. *Gazz. Chim. Ital.* **1972**, *102*, 1026.
(8) Bombieri, G.; Degetto, S.; Forsellini, E.; Marangoni, G.; Immirzi, A. *Cryst. Struct. Commun.* **1977**, *6*, 115.
(9) Syper, L.; Kloc, K.; Mlochowski, J.; Szulc, Z. *Synthesis* **1979**, 521.

0020-1669/85/1324-2763$01.50/0